Hindawi
Advances in Civil Engineering
Volume 2022, Article ID 9446398, 17 pages
https://doi.org/10.1155/2022/9446398

Research Article

Analysis of Rational Finite Element Model of Two-Span Skew Girder Bridge Based on Shaking Table Test

Ying Huang[1] **and Yongji Xu**[2]

[1]*Fujian Chuanzheng Communications College, Fujian Fuzhou 350007, China*
[2]*Fujian Traffic Construction Engineering Test and Detection Co., Ltd,, Fujian Fuzhou 350008, China*

Correspondence should be addressed to Ying Huang; huangying6820@163.com

Received 18 March 2022; Accepted 11 May 2022; Published 7 June 2022

Academic Editor: Jian Ji

Based on the shaking table test, the seismic responses of the main parameters of the two-span skew bridge were gutted. The finite element model of the test model was established by the finite element analysis software OpenSEES. An improved model of single beam quality distribution was proposed. The stiffness of the end beam of the improved single beam model was twice that of the actual end beam, rather than the rigid arm. At the same time, the main beam mass was distributed in the way that the single beam shares half and the beams at both ends share half, taking into account the torsion of the beam body. Three-direction ground motion input analysis was carried out to improve the quality distribution model of the single beam, and the seismic response of the structure under the three-direction ground motion input was obtained, and the comparison was made between the analytical results and experimental results. The results show that the improved single beam quality distribution model can consider the torsion effect of the beam, while the result of the analysis was greatly improved, which was more close to the experimental value, and could greatly improve the efficiency of the calculation.

1. Introduction

In recent years, skew girder bridges have been widely used in high-grade highways, crowded urban areas, and interchange structures at home and abroad because skew girder bridges can better meet the alignment requirements of route design, shorten the route to save investment, and improve economic benefits [1, 2]. At present, most scholars analyze the dynamic characteristics of skew bridges only by using the finite element model for seismic response analysis [3–8]. Due to the lack of experimental support, the analysis of the accuracy and rationality of the finite element model is relatively lacking.

Three models are mainly used to simulate the main beam by OpenSEES, such as the single beam, double beam, and multibeam model. The beam grid method of the multibeam model is the most widely used [9, 10], while the single beam model is relatively simple and computationally efficient [11]. Meng and Lui [12, 13] used double beams to simulate the main girder by considering the true boundary conditions of the bridge.

The reasonable modeling method of the main beam and support of the skew beam bridge was analyzed based on the shaking table test of two-span continuous skew bridge. At the same time, the bearing model unit type was also analyzed, and the reasonable main beam and bearing model unit were selected. Finally, the seismic response analysis results of the model were compared with the experimental results to verify the correctness of the modeling method and the rationality of the finite element model.

2. Finite Element Model Establishment

The finite element model of the skew bridge established in this paper was consistent with the experimental model [14–16]. The specific geometric parameters and material parameters as well as the main material mechanical indexes of the model are shown in Tables 1 and 2.

Table 1: Geometrical dimensions and material parameters.

Name	Geometric size	Longitudinal reinforcement	Stirrup	Concrete	Change parameter
Bridge deck	Total length: 10.4 m; net span length: 5 m width: 2.1 m; thick: 0.25 m	HRB335Ø14	HPB235Ø10	C30	Skew angle: 15°, 30°, 45°
Cover beam	Width: 0.7 m; height: 0.35 m	HRB335Ø16	HPB235Ø10	C25	Skew angle: 15°, 30°, 45°
Pier	Diameter: 0.25 m	HRB335Ø10	HPB235Ø6	C25	Pier height: 0.5 m, 1 m, 1.5 m Clamping ratio: 0.2%, 0.4%, 0.6%
Support	Round plate rubber bearing: 200 * 35				

Table 2: Main material mechanics index of the skew bridge model.

Material	Reinforcement diameter	Yield strength (MPa)	Tensile strength (MPa)	Elongation
Reinforcement	6 mm	360	560	0.33
	8 mm	320	530	0.32
	10 mm	330	550	0.32
	12 mm	355	540	0.31
	14 mm	380	500	0.33
	16 mm	385	515	0.31
Material	Label	Compressive strength (MPa)	Elastic modulus (×104 MPa)	
Concrete	C30	35.2	2.542	
	C25	29.3	2.85	
Material	Model	X-direction stiffness (kN/m)	Y-direction stiffness (kN/m)	Z-direction stiffness (kN/m)
Support	200 ∗ 35	797694	1507.2	1507.2

This section simulates the test model with OpenSEES by referring to relevant literatures at home and abroad. The establishment of each component of the model can be found in literature [14].

2.1. Main Beam. Previous earthquake damage surveys have shown that the seismic damage of the main beam of skew beam bridge is small under the action of earthquake and basically remains linear elasticity. Therefore, the elastic three-dimensional beam element was used for simulation, and the later counterweight was considered by converting it into mass.

2.2. Laminated Rubber Bearing. The hysteresis curve of plate rubber bearing is narrow and long strip, which is generally approximate to linear elasticity in numerical analysis [17, 18]. Combined with the Detailed Rules for Anti-Seismic Design of Highway Bridges [19], in OpenSEES finite element simulation, unixism material elastic materials were selected for simulation. The stiffness value of plate rubber bearing calculated according to the specification [20] is listed in Table 2.

2.3. Piers and Bent Caps. In this paper, fiber element was used to simulate pier and cap beam. The fiber element can consider the influence of the internal force of the section beyond the bending moment on the structural failure and can consider the two-way bending deformation, which can better simulate the response of the structure in the elastic-plastic state under earthquake [21–23].

2.4. Abutment. In previous destructive earthquakes, the damage degree of the abutment of skew bridge is generally small. Therefore, the abutment structure can be assumed to be rigid, and the joints under the bearing can be directly consolidated in the simulation.

2.5. Reinforced Concrete. There are three main types of materials: reinforced materials, confined concrete materials, and nonconfined concrete materials. In this paper, the concrete 02 material in OpenSEES was selected to simulate the confined concrete and nonconfined concrete, and the steel 02 material was selected to simulate the reinforcement.

2.5.1. Concrete 02 Material Model. The concrete 02 material model can not only consider the restraint effect of transverse stirrups on concrete but also consider the residual strength of concrete. Kent–Scott–Park constitutive is adopted for the compression section of the model [24]. The peak stress and strain of the compression curve and the slope of the softening section are mainly considered. The tensile section mainly considers the tensile hardening of concrete and the stiffness degradation effect after the initial cracking. In terms of unloading, the stress-strain relationship of the model is determined according to the modified Karsan–Jirsa unloading rule proposed by Taucer et al. [25]. The expression of the model is as follows:

$$\sigma_c = \begin{cases} Kf_c'\left[2\left(\dfrac{(\varepsilon_c/\varepsilon_0)\varepsilon_c}{\varepsilon_0}\right) - \left(\dfrac{\varepsilon_c/\varepsilon_0\varepsilon_c}{\varepsilon_0}\right)^2\right], & \varepsilon_c \le \varepsilon_0, \\ Kf_c'[1 - Z(\varepsilon_c - \varepsilon_0)], & \varepsilon_0 \le \varepsilon_c \le \varepsilon_{20}, \\ 0.2Kf_c', & \varepsilon_c > \varepsilon_{20c}, \end{cases} \quad (1)$$

where

$$\varepsilon_0 = 0.002K,$$

$$K = 1 + \frac{\rho_s f_{yh}}{f_c'}, \quad (2)$$

$$Z = \frac{0.5}{(3 + 0.29f_c'/145f_c' - 1000) + 0.75\rho_s\sqrt{(h'/s_h)} - 0.002K},$$

ε_0 is the strain corresponding to the maximum stress of concrete, ε_{20} is the residual strain corresponding to residual stress of concrete (20% of maximum stress), K is the increase coefficient of stirrup, Z is the slope corresponding to strain softening, f_c' is the maximum stress of concrete, f_{yh} is the yield strength of stirrup, ρ_s is the volume stirrup ratio, h' is the concrete core width, and s_h is the stirrup spacing.

When the stirrup breaks, the concrete will lose its restraint effect, resulting in a sudden decrease in the stress-strain curve of the confined concrete. Priestle and Seible gave a conservative estimate of the ultimate strain of the reinforcement [26]:

$$\varepsilon_{\max} = 0.004 + 0.9\rho_s\frac{f_{yh}}{300}. \quad (3)$$

In the concrete 02 material model, the tension section is the rising straight line section and the falling straight line section, and the maximum tensile stress and softening stiffness are as follows:

$$f_t' = -0.14Kf_c', E_{ts} = \frac{f_t'}{0.002_{ts}}. \quad (4)$$

2.5.2. Steel 02 Material Model. Steel 02 material model is the modified Giuffre–Menegotto–Pinto model [15], which can better simulate the deformation characteristics of reinforcement, and its expression is as follows:

$$\sigma^* = b\varepsilon^* + \frac{(1-b)\varepsilon^*}{\left(1 + \varepsilon^{*R}\right)^{1/R}}, \quad (5)$$

where $\varepsilon^* = (\varepsilon - \varepsilon_r/\varepsilon_0 - \varepsilon_r)$ and $\sigma^* = (\sigma - \sigma_r/\sigma_0 - \sigma_r)$, ε_r is the strain corresponding to reverse loading point, σ_r is the stress corresponding to reverse loading point, ε_0 is the strain corresponding to the intersection of the initial asymptote and the asymptote after yield, and σ_0 is the stress corresponding to the intersection of the initial asymptote and the asymptote after yield.

2.6. Collision Element. In this paper, the double broken line proposed by Muthukumar and DesRoches was used to simulate the collision stiffness and simplify the collision model [27]. There are special collision elements in OpenSEES to simulate the double broken line model proposed by Muthukumar. The commands to define the model in OpenSEES are as follows:

Uniaxial Material Impact Material $matTag $K1 $K2 $$\delta y$ $gap

Therein, $K1 is the initial stiffness; $K2 is the impact stiffness

$$\delta y$ is the yield displacement

$gap is the initial clearance

K1, K2, δy, and δm are calculated by energy loss.

The energy dissipation during collision is expressed as follows:

$$\Delta E = \frac{k_h\delta_m^{n+1}\left(1 - e^2\right)}{n+1}, \quad (6)$$

where k_h is the stiffness of the main beam, taken as EA/L; $n = 1.5$; e is defined as the recovery coefficient, with a value range of 0.6~0.8; δ_m is the maximum penetration displacement allowed in the collision process, and K_{eff} is the effective stiffness. The values of each parameter are as follows:

$$K_{\text{eff}} = k_h\sqrt{\delta_m},$$

$$\delta_y = a\delta_m,$$

$$K1 = K_{\text{eff}} + \frac{\Delta E}{a\delta_m^2}, \quad (7)$$

$$K2 = K_{\text{eff}} - \frac{\Delta E}{(1-a)\delta_m^2}.$$

The specific values applied to the simulation of the project are shown in Table 3.

3. Reasonable Finite Element Model Analysis

3.1. Reasonable Finite Element Model Analysis of Main Beam. The test takes the typical two-span continuous skew beam bridge of highway as the research object. The skew angle is taken as 15°, 30°, and 45°, respectively. According to the similarity coefficient, the total length of the model bridge is determined to be 10.4 m. The two spans are arranged continuously with equal span, the bridge width is 2.1 m, and the slab thickness is 0.25 m; the reinforced concrete double column circular pier is set in the middle, and there are abutments on both sides. The shaking table test in the laboratory was carried out. The field test photos are shown in Figure 1, and a series of test results are obtained.

Table 3: Collision element parameters and corresponding values.

Parameter	Value
k_h	5.42×10^9 Pa
n	1.5
e	0.8
δ_m	25.4 mm
a	0.1
δ_y	2.54 mm
K_{eff}	8.64×10^8 Pa
$K1$	10.38×10^8 Pa
$K2$	3.85×10^8 Pa

Figure 1: Site test photo.

In finite element analysis, the single beam, double beam, and multibeam models were used to simulate the main beam, and the full bridge model was established, respectively (Figure 2). The seismic response analysis of the full bridge model was carried out to obtain the acceleration response, displacement response, acceleration response, and displacement of the bridge deck and the internal force response of the support. All of these responses were compared with the test results to explore the accuracy of the finite element model.

3.2. Input Ground Motion Selection. The research shows that under the influence of different ground motions, the seismic response of bridge structures is often very different, some even several times or even more than ten times. Therefore, the reasonable selection of ground motion is very important for the research of test and finite element simulation.

The selection of input ground motion mainly considers three factors [28, 29]: seismic amplitude, spectral characteristics, and duration of ground motion. In order to better reflect the randomness of the input ground motion, five typical ground motions and a total of 20 ground motion records were selected from each of the four types of sites (Table 4).

The 20 ground motion spectra selected in the simulation were evenly distributed, and the correlation coefficients calculated according to formula (8) are less than 0.1, meeting the requirements of the current code [19].

$$|\rho| = \left| \frac{\sum_j a_{1j} a_{2j}}{\sqrt{\sum_j a_{1j}^2} \sqrt{\sum_j a_{2j}^2}} \right|. \tag{8}$$

3.3. Seismic Response Analysis

3.3.1. Acceleration Response Analysis. It can be seen from the comparison of the acceleration responses in Figures 3–5 that the overall longitudinal acceleration responses of the left and right ends of the three model bridge decks are consistent with the experimental values under the action of longitudinal seismic waves. The longitudinal acceleration response of the multibeam model bridge deck is closer to the experimental value. The calculated values of the double beam model and the single beam model are similar. The three models have the same acceleration response of the left end, the right end, and the top of the bridge deck under the action of the transverse seismic wave and the two-way seismic wave. The overall trend is consistent with the experimental value.

3.3.2. Displacement Response Analysis. It can be seen from the comparison of the displacement responses in Figure 6 that the overall longitudinal displacement response of the right end of the three model bridge decks is consistent with

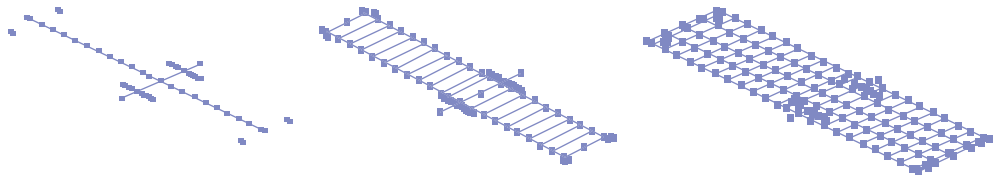

(a) (b) (c)

Figure 2: Full bridge finite element model. (a) Single beam. (b) Double beam. (c) Multi-beam.

Table 4: Ground motion records of various sites.

I site	II site	III site	IV site
Gansu seismic wave	WHITTIER wave	El-Centro wave	Loma-Prieta wave
Chi-chi wave	Parkfield wave	Wenchuan seismic wave	Landers wave
Wenchuan seismic wave	Tangshan seismic wave	Kobe wave	Chi-chi wave
Tangshan array wave	San Fernando wave	Northridge wave	Whittier narrows wave
Loma Prieta wave	Landers wave	Imperial valley wave	Tangshan array wave

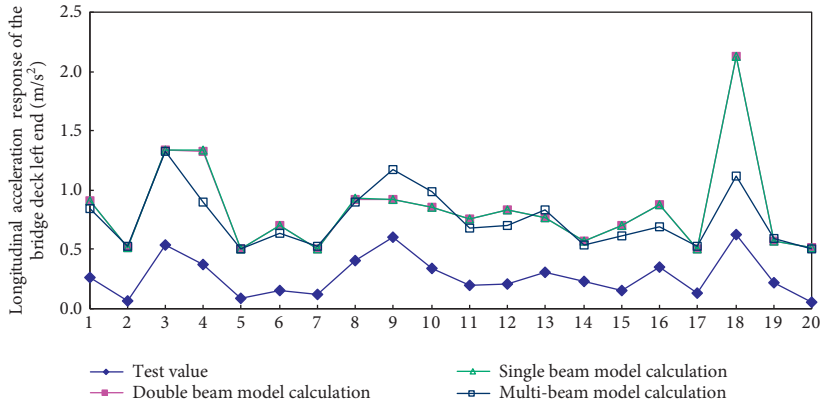

(a)

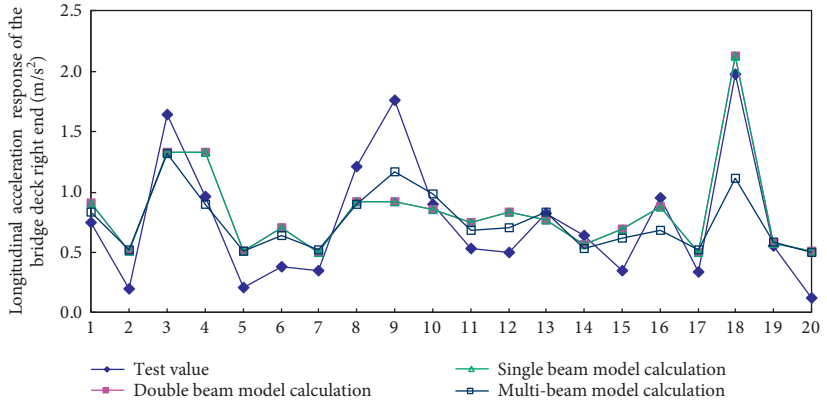

(b)

Figure 3: Continued.

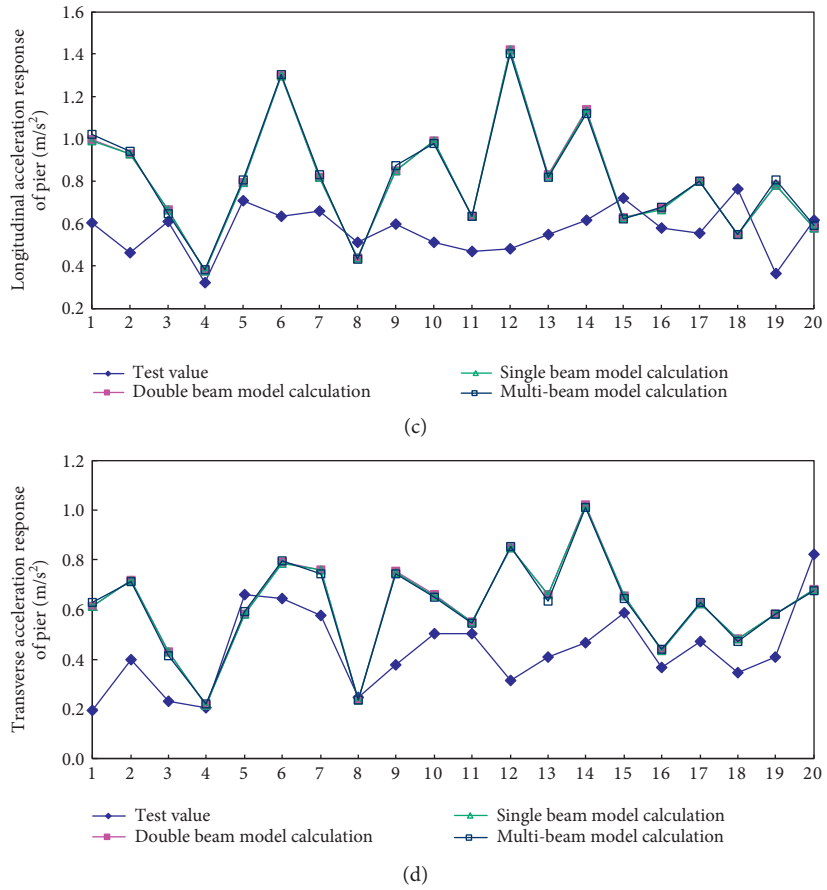

Figure 3: Acceleration response under longitudinal seismic waves. (a) Left end of bridge deck. (b) Right end of bridge deck. (c) Longitudinal acceleration response of pier. (d) Transverse acceleration response of pier.

the experimental values under the action of longitudinal seismic waves. The longitudinal displacement response of the multibeam model bridge deck is closer to the experimental value. The calculated values of the double beam model and the single beam model are similar. The three models have the same displacement response of the right end of the bridge deck under the action of the transverse seismic wave and the two-way seismic wave. The overall trend is consistent with the experimental value.

3.3.3. Internal Force Response Analysis. Figure 7 is a schematic diagram of the bearing position of the test model of the two-span skew girder bridge. It can be seen from the comparison of the internal force responses of the four supports at the left end of the bridge deck under the action of the two-way seismic wave in Figures 8–10. The longitudinal internal force responses of the four supports at the left end of the three models are basically the same under the action of longitudinal seismic waves. The lateral internal force responses of the single beam model and the double beam model are similar but larger than the multibeam model, with a difference of about 25%. The obvious difference is reflected in the vertical internal force response. The vertical internal force response of the four supports of the single beam model is close to 25 kN, while the vertical internal forces of the double beam model and the multibeam model are quite different. The main reason is that the double beam model and the multibeam model can consider the torsional effect of the beam body, while the single beam model ignores.

From the comparative analysis of the seismic response results and test results of the three models under the action of 20 kinds of seismic waves, it can be seen that the multibeam model can react to the actual test situation. However, due to the large number of units, the calculation takes 5 times longer than the double-beam model, and the calculation efficiency is low. The double beam is used to simulate the bridge deck. Compared with the simple beam element in the past, the double beam element can consider the torsional effect of the skew bridge deck. The double beam model can obtain the response characteristics under earthquake action [12], and the results are close to the results of complex finite element analysis models. The single beam model is a simplification to improve the calculation efficiency [11], and the calculation efficiency is three times that of the double beam model. From the analysis results, the acceleration response and displacement response of the model are consistent with the double beam model. The shortcoming is that it cannot simulate the torsional effect, and the internal force response also has a large deviation compared with the multibeam model. The analysis efficiency of the real bridge is low if multibeam or double-beam model is adopted. Therefore,

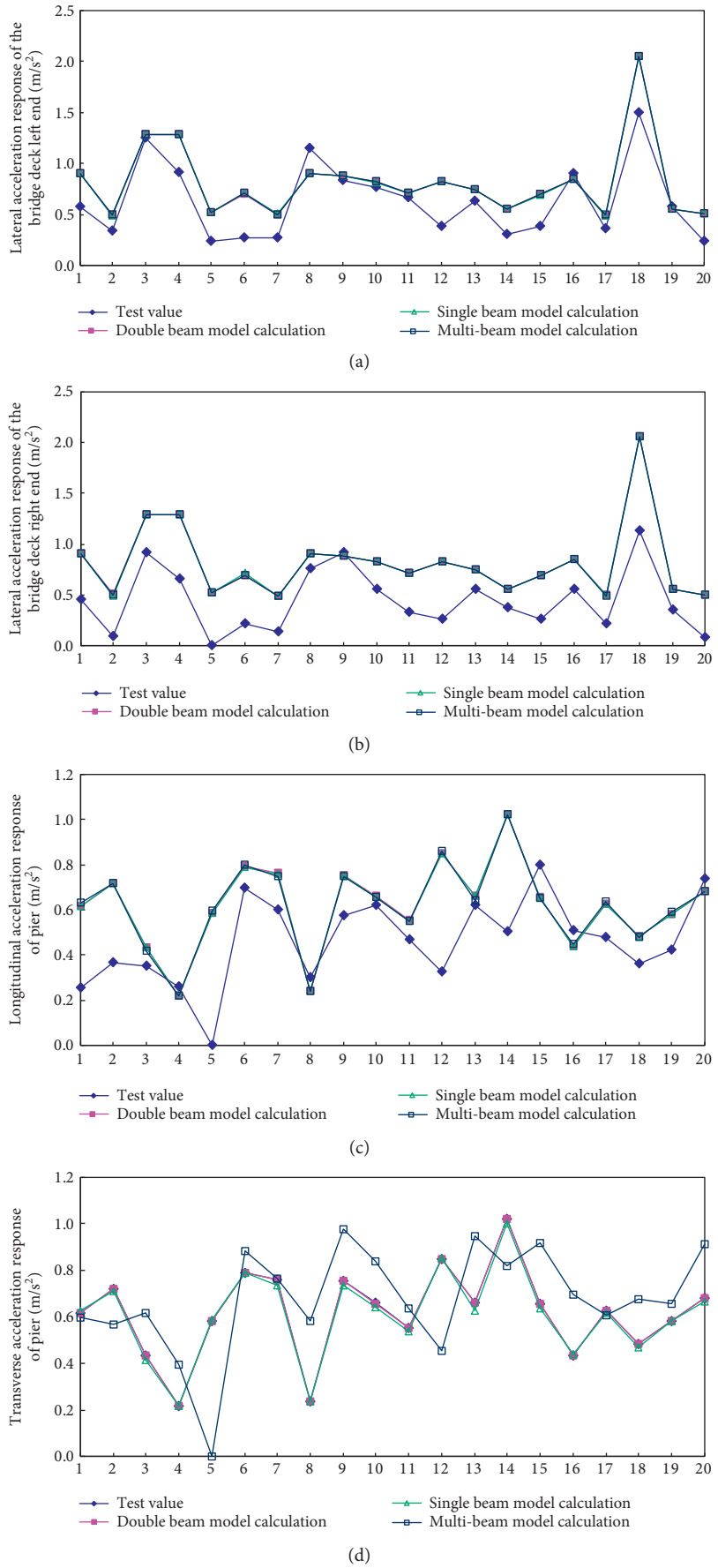

Figure 4: Acceleration response under transverse seismic waves. (a) Left end of bridge deck. (b) Right end of bridge deck. (c) Longitudinal acceleration response of pier. (d) Transverse acceleration response of pier.

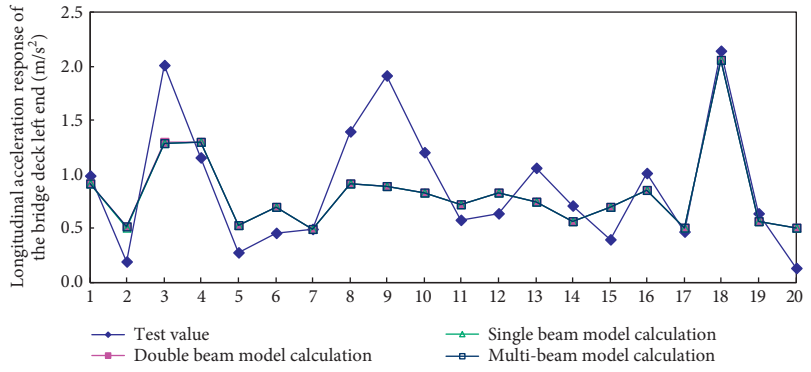

(a)

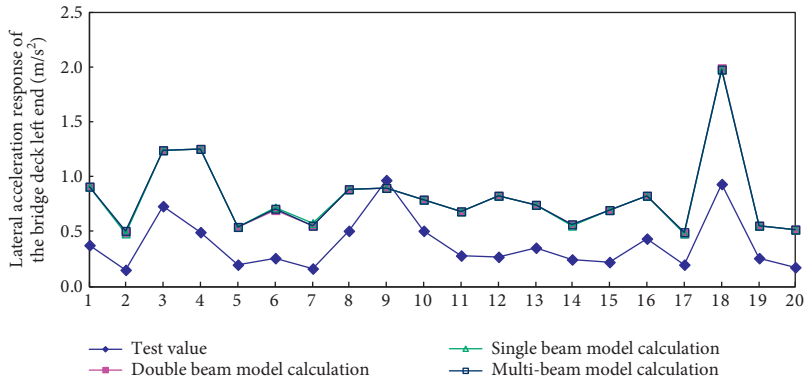

(b)

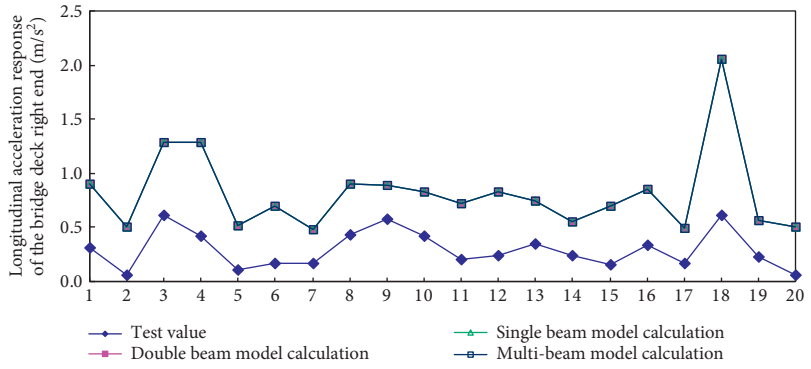

(c)

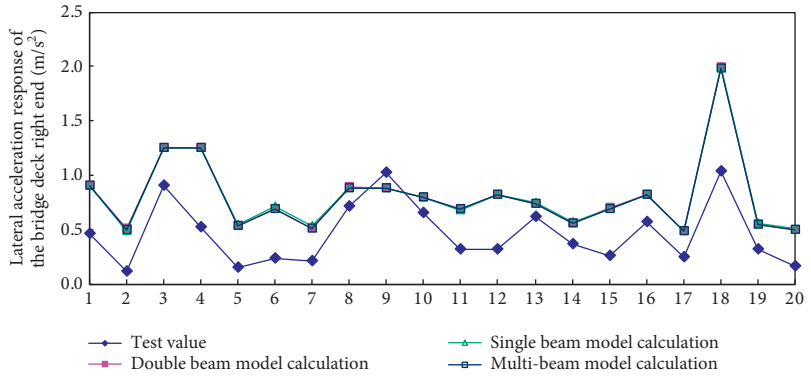

(d)

Figure 5: Continued.

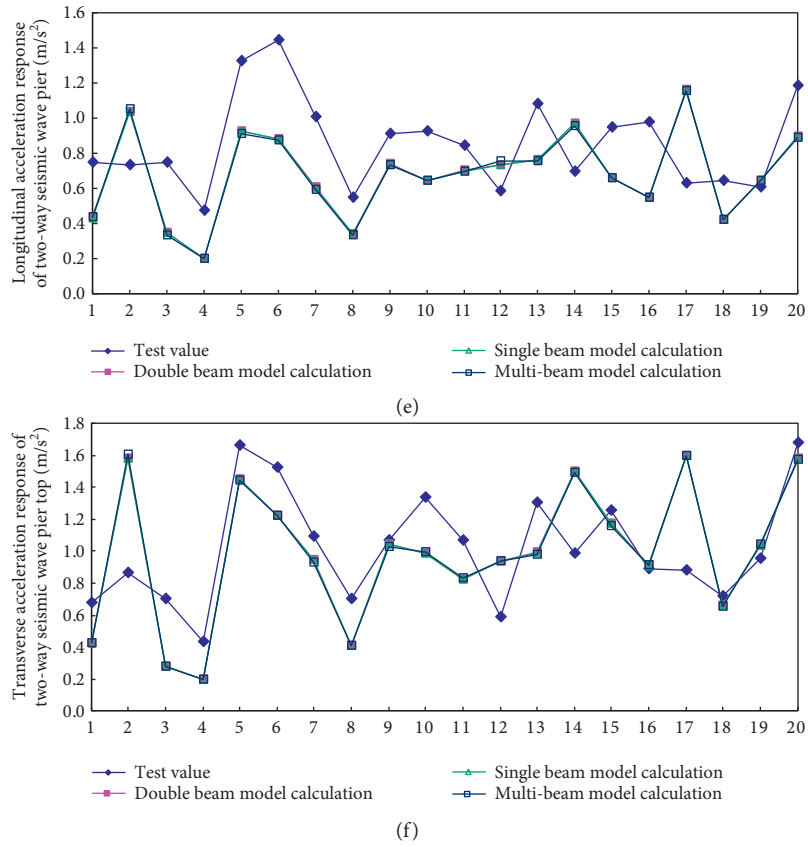

FIGURE 5: Acceleration response under the action of two-way seismic waves. (a) Bridge deck left end portrait. (b) Bridge deck left end lateral. (c) Bridge right side portrait. (d) Bridge right side horizontal. (e) Pier top portrait. (f) Pier top horizontal.

how to improve the single beam model can not only improve the simulation results but also greatly improve the calculation efficiency. Based on this idea, this paper proposes an improved single beam mass distribution model, which is named the beam end mass distribution model.

4. Determination of the Improved Finite Element Model for Single Beam Mass Distribution

In the existing analysis [10, 11], the rigid arm (without mass) is used at the beam end to realize the connection between the support, and the main beam is simulated by the elastic three-dimensional beam unit, as shown in Figure 11(a). The model has the following problems in the actual calculation:

(1) The main beam mass is concentrated on a single beam, which is difficult to reflect the torsion of the main beam.

(2) In the actual structure, the beam end is not completely rigid. This makes it easier to make the reaction force distribution of the beam end support extremely uneven when the main beam has a large skew angle. Even the bearing is suspended at the acute angle.

Based on this, the article proposes a single beam system model as shown in Figure 11(b), which differs from the previous models in the following ways:

(1) The end beam stiffness is twice the stiffness of the actual end beam, rather than the rigid arm

(2) The main beam is divided into a single beam and half-shared

In order to compare the two mass distribution models, two main beam mass distribution models are established, respectively, and the displacement seismic response analysis of the structure is obtained. The EI-centro wave is selected. The seismic wave input adopts the same X-direction input as the test. The skew beam model with a skew angle of 30° and the displacement response results were compared with the experimental values. The analysis results are shown in Table 5.

It can be seen from Table 5 that the longitudinal response of the model proposed in this paper is close to the experimental value, especially when the peak value of seismic wave acceleration is 0.1 g and 0.2 g, the error with the experimental value can reach 6%. The value error reaches 21.5% under the lateral displacement response. However, the longitudinal displacement response and lateral displacement response of the model established according to the mass distribution of the main beam are greatly different from the experimental

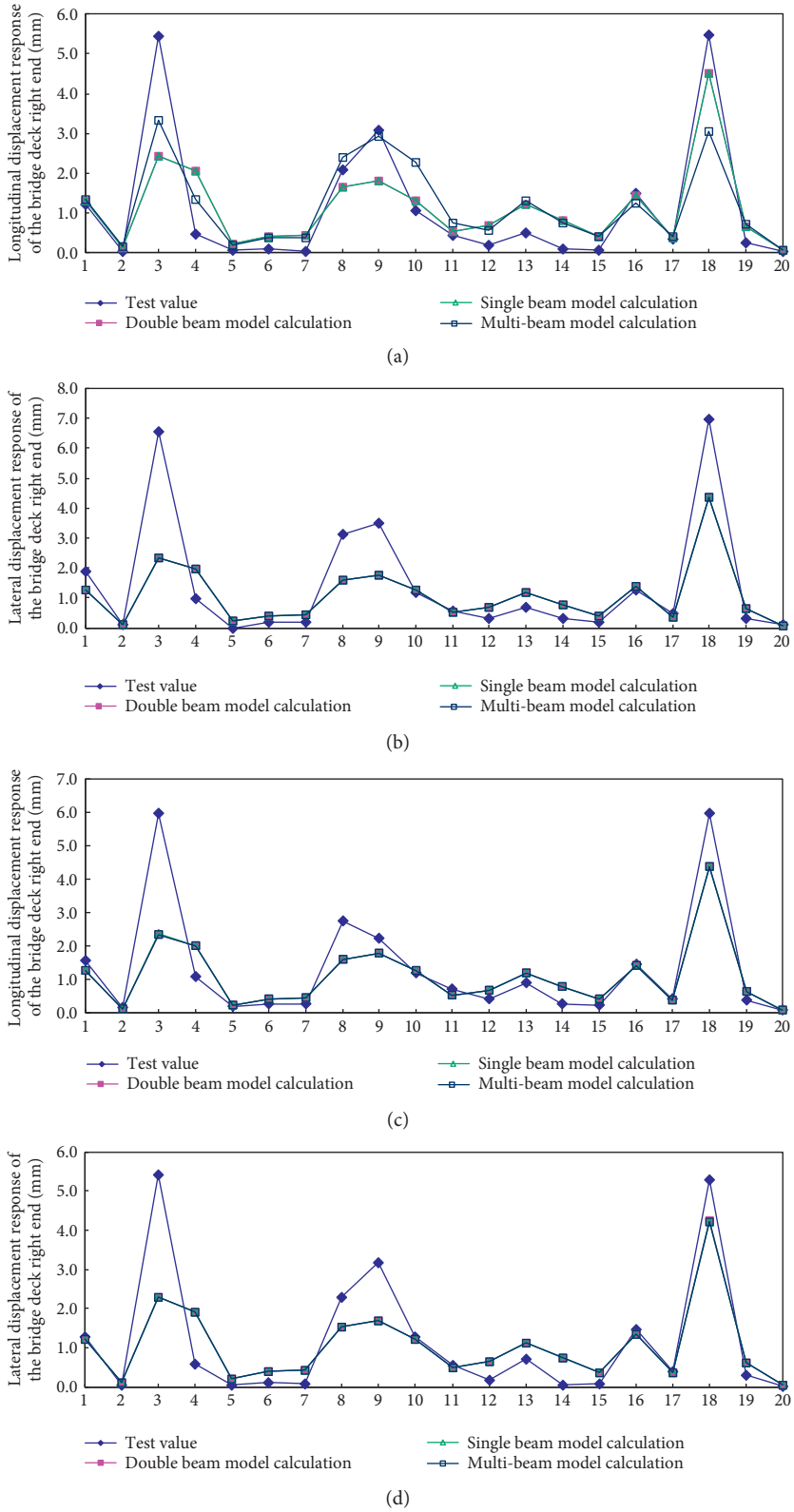

Figure 6: Displacement responses of the right end of the bridge deck. (a) Longitudinal response under longitudinal seismic waves. (b) Lateral response under transverse seismic wave. (c) Longitudinal response under the action of two-way seismic wave. (d) Lateral response under the action of two-way seismic wave.

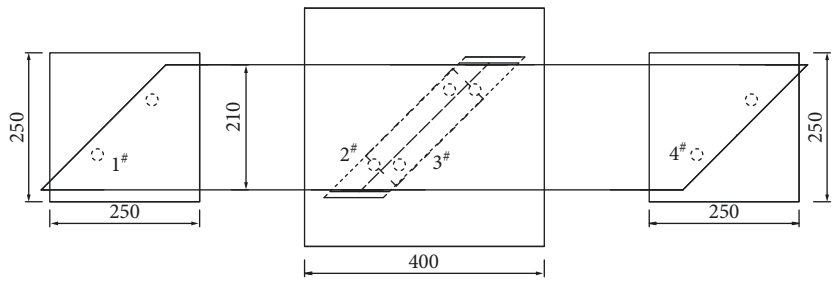

Figure 7: The bearing layout of two-span skew girder bridge test model schematic diagram.

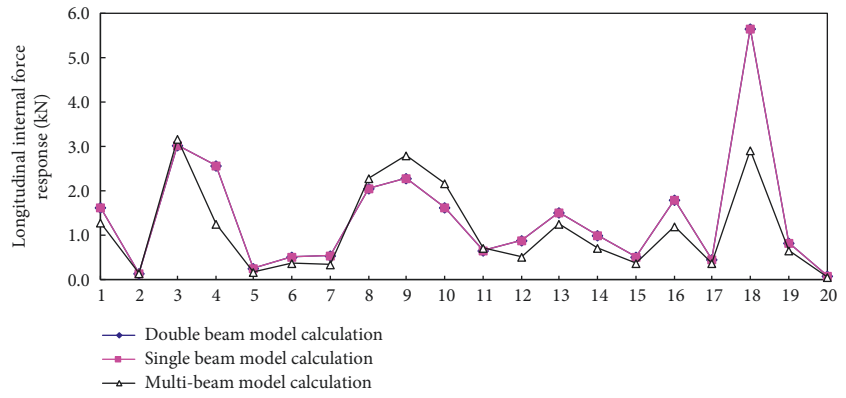

(a)

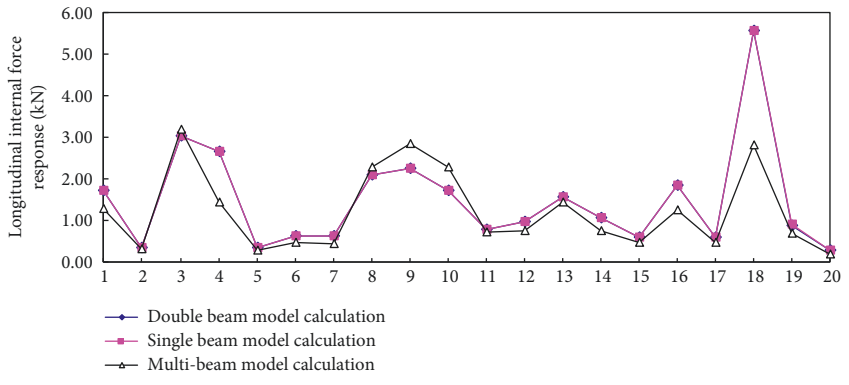

(b)

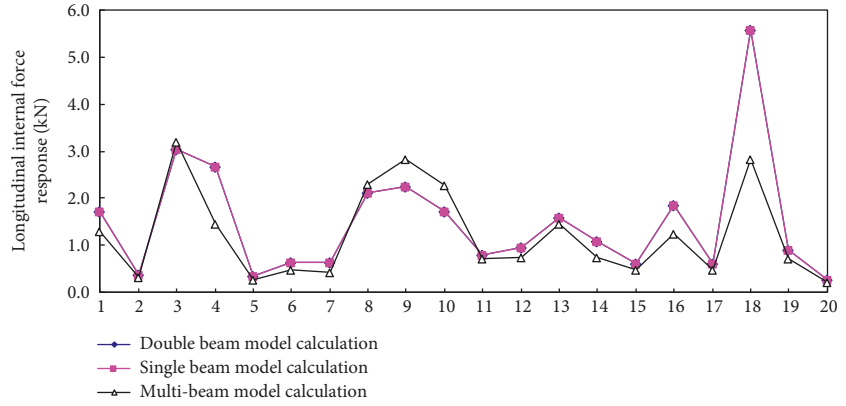

(c)

Figure 8: Continued.

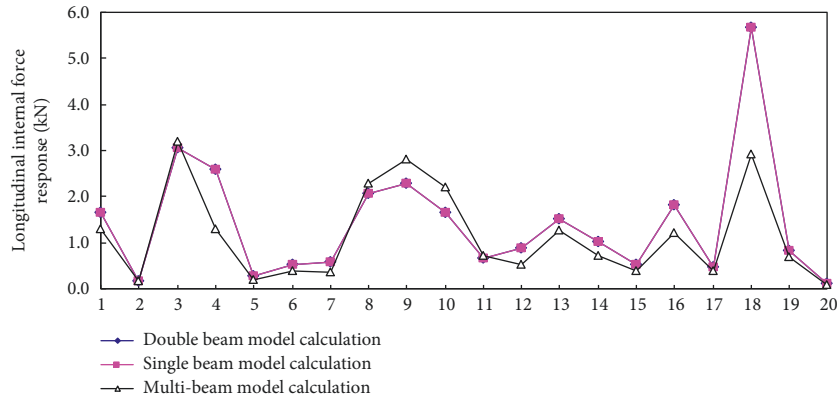

(d)

Figure 8: Support longitudinal internal force response. (a) No. 1 support. (b) No. 2 support. (c) No. 3 support. (d) No. 4 support.

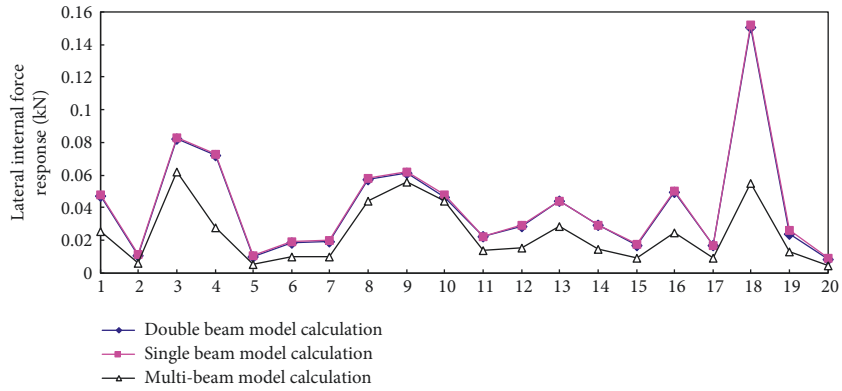

(a)

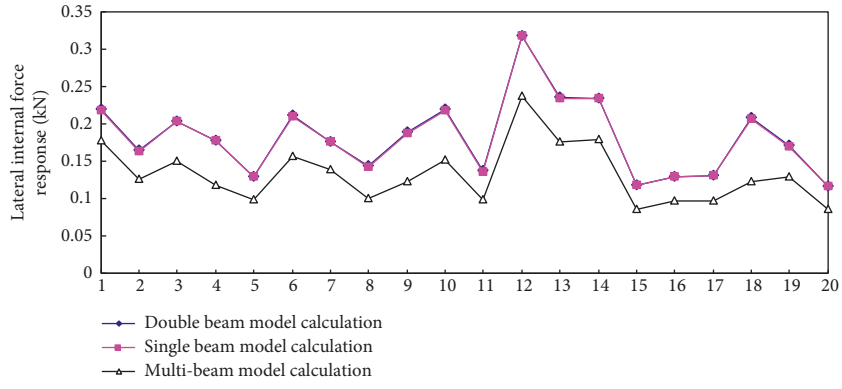

(b)

Figure 9: Continued.

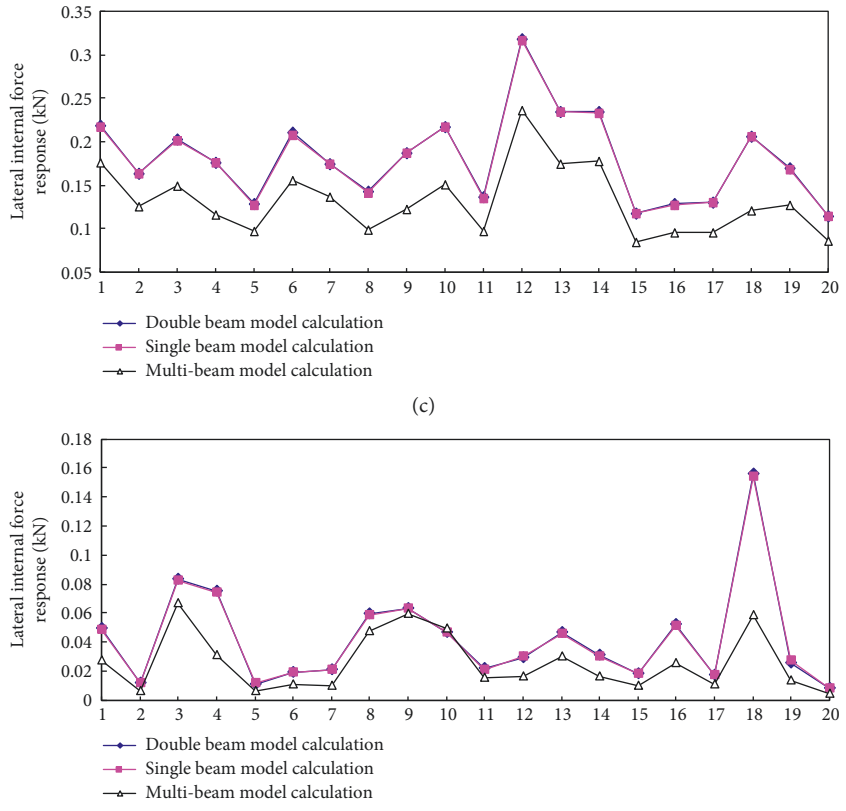

Figure 9: Lateral internal force response of the support. (a) No. 1 support. (b) No. 2 support. (c) No. 3 support. (d) No. 4 support.

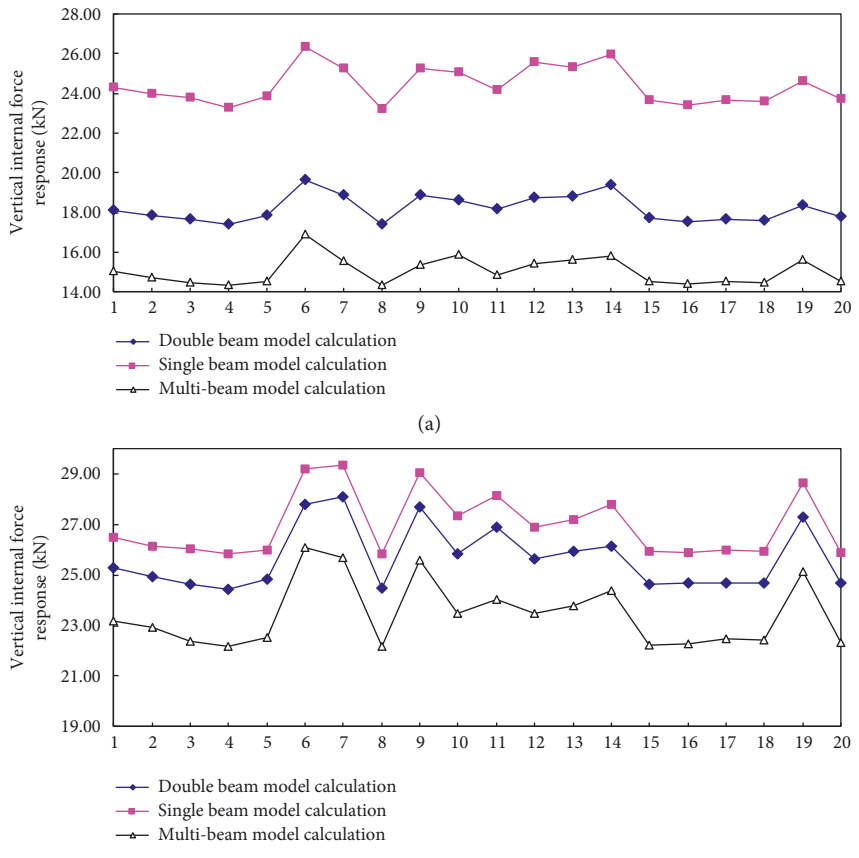

Figure 10: Continued.

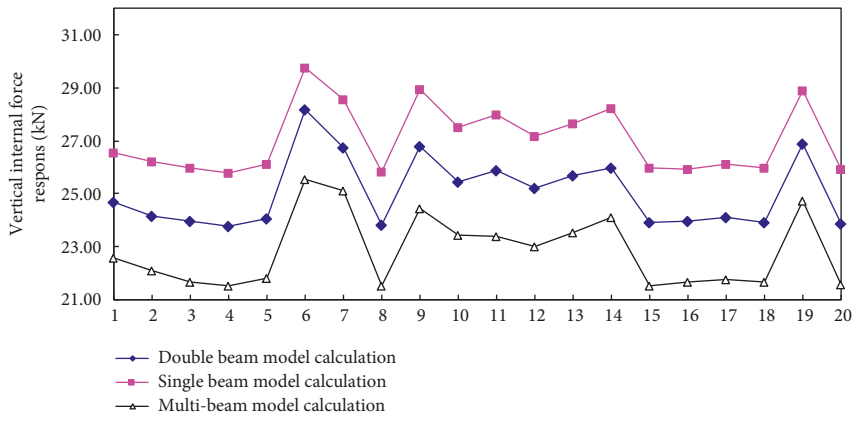

(c)

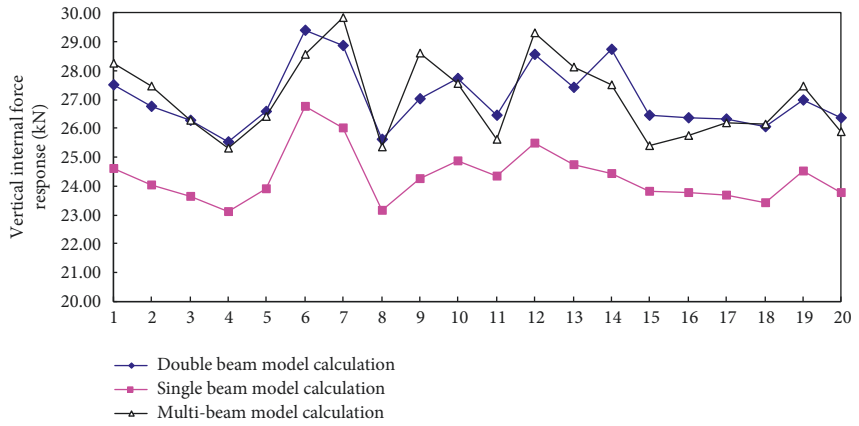

(d)

Figure 10: Vertical internal force response of the support. (a) No. 1 support. (b) No. 2 support. (c) No. 3 support. (d) No. 4 support.

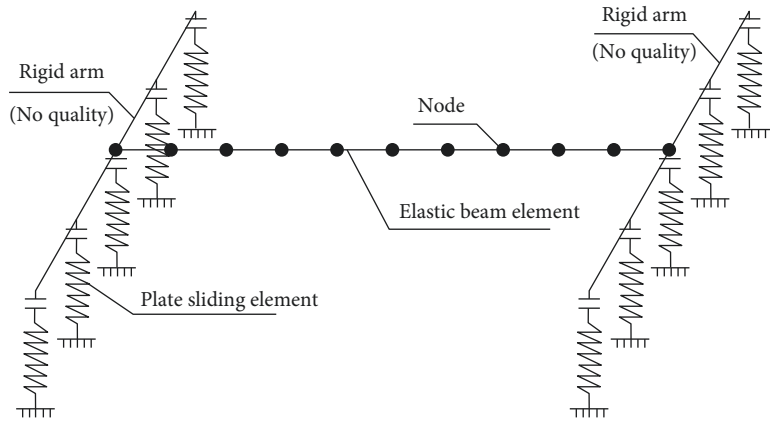

(a)

Figure 11: Continued.

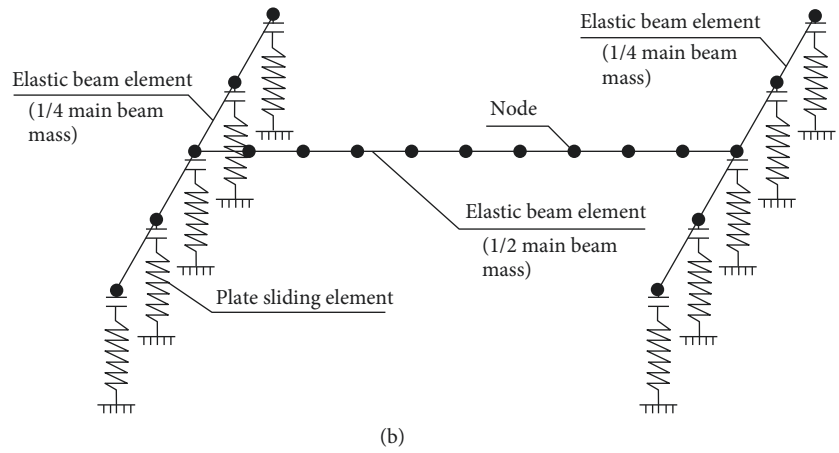

Figure 11: Main beam mass distribution model. (a) Conventional single beam model. (b) Improved single beam model.

Table 5: Main beam displacement response result.

Displacement direction	Seismic wave acceleration peak (g)	Displacement response of different mass distribution simulation types (mm)			Error (%)	
		Main beam concentration quality Δ_1	Beam end distribution quality Δ_2	Test value Δ_3	$(\Delta_1 - \Delta_3)/\Delta_3$	$(\Delta_2 - \Delta_3)\Delta_3$
Portrait	0.1	2.323	3.525	3.573	34.1	1.34
	0.2	4.645	7.958	8.438	45.0	5.69
	0.3	6.967	12.200	13.816	50.0	11.7
Landscape	0.1	$2.89395e-2$	0.577	0.710	71.8	18.7
	0.2	$5.75105e-2$	0.815	1.026	61.0	20.6
	0.3	$8.70727e-2$	1.287	1.639	63.3	21.5

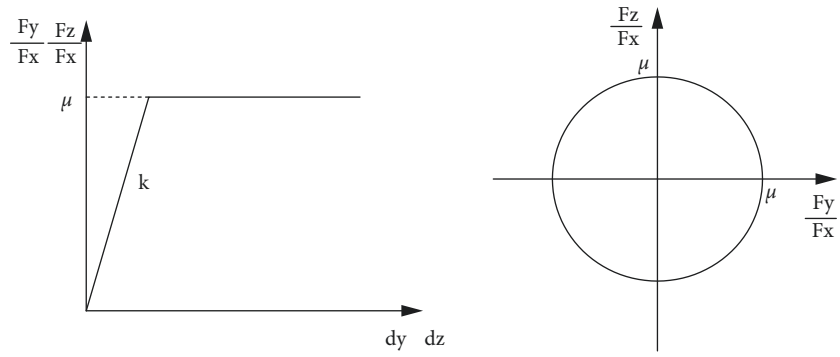

Figure 12: Slab-slip unit stress-strain curve.

values, both exceeding 30%. The analysis indicates that the end mass distribution model proposed in this paper is more accurate than the original main beam mass distribution model.

5. Determination of Reasonable Finite Element Model of Bearing

At present, the element zero length is generally selected for the bearing simulation in OpenSEES. The zero-length unit is mainly using different material constitutive implementations. The elastic phase mainly used the uniaxial material elastic to simulate for the ordinary rubber bearing. When studying the nonlinear phase of the bearing, the reinforced material (uniaxial Material Steel 01) is usually used to simulate, and the relative slip of the bearing is simulated by setting the yield value of the reinforcing bar. In this paper, the flat slider bearing was selected to simulate the support. The stress-strain curve of the unit is shown in Figure 12.

In order to compare the simulation results of the two types of bearing units, the displacement seismic response analysis of the structure is carried out by using two kinds of unit simulation supports. The seismic wave selection is the same as the EI-centro wave, and the seismic wave input adopts the same X-direction input as the test. The analysis results are shown in Table 6. It can be seen from the table that the simulation results using the plate slip unit are close to the experimental values, and the error is within 6%, but the

Table 6: Main beam displacement response result.

Seismic wave acceleration peak (g)	Displacement response of different bearing simulation types (mm)			Error (%)	
	Ordinary support (zero length unit) Δ_1	Sliding bearing (flat slip unit) Δ_2	Test value Δ_3	$(\Delta_1 - \Delta_3)/\Delta_3$	$(\Delta_2 - \Delta_3)/\Delta_3$
0.1	1.026	0.896	0.897	14.38	0.11
0.2	2.052	1.468	1.489	37.81	1.41
0.3	3.072	2.020	1.919	60.08	5.26

result of zero-length unit simulation is large. The analysis results show that it is more accurate to use the plate slip unit to simulate the bearing.

6. Concluding Remarks

In this paper, based on the shaking table test of two-span continuous skew beam bridge, the experimental model was used as the modeling basis, and the reasonable modeling method of the main beam and the support was analyzed. Comparing the results of the finite element analysis with the test results, the following conclusions are obtained:

(1) Three kinds of main beam models of single beam, double beam, and multibeam were established by using the finite element analysis software OpenSEES. It can be seen from the comparison of seismic response results and test results of three models under the action of 20 kinds of seismic waves. The acceleration response of the beam is basically the same, and the displacement response of the multibeam model is closer to the experimental value. The displacement response of the double beam and the single beam model is basically the same, and the displacement response value of the multibeam model differs by about 10%. The vertical internal force response of the four supports of the single beam model is close, while the vertical internal forces of the four supports of the double beam model and the multibeam model are quite different mainly because the double beam model and the multibeam model can consider the torsion of the beam body while the single beam model ignores the torsion.

(2) An improved single beam main beam mass distribution model is proposed. The model can consider the torsional effect of the beam. When the seismic wave is input longitudinally, the maximum error of the longitudinal displacement response of the main beam and the experimental value is about 11.7%. The maximum contrast error is about 21.5% of the lateral displacement response, which is much better than the original main beam mass concentration model analysis result, which is closer to the experimental value and can greatly improve the calculation efficiency.

(3) The flat sliding unit was used to simulate the bearing by comparing with the commonly used zero-long unit. The maximum error is about 5.26% of the longitudinal displacement response, but zero-long unit simulation results error can reach 60.08%. All are compared with the test value which indicates that it is more accurate to use the flat slip unit to simulate the support of the skew beam bridge.

Data Availability

The data used to support the findings of this study are available from the corresponding author upon request.

Conflicts of Interest

The authors declare that they have no conflicts of interest.

Acknowledgments

This work was financially supported by the National Youth Science Foundation of China: Research on seismic damage mechanism and seismic design of skew beam bridge based on shaking table test (Grant No. 51208112), the Application Technology Collaborative Innovation Center Project of Fujian Provincial Department of Education (Grant No. [2018]105), the Transportation Science and Technology Project of Fujian Provincial Department of Communications (Grant No. 202033), and the Fund for Doctoral Research Launch Project of Fujian Chuanzheng Communications College (Grant No. 20200302).

References

[1] Z. Wei-dong and S. Guan-ping, "Earthquake resistance status of highway skew beam bridge," in *ProceThe 4th National Symposium on Earthquake Disaster Reduction Engineering*, pp. 414–422, Beijing, China, October 2009.

[2] E. Omranian, A. E. Abdelnaby, and G. Abdollahzadeh, "Seismic vulnerability assessment of RC skew bridges subjected to mainshock-aftershock sequences," *Soil Dynamics and Earthquake Engineering*, vol. 114, pp. 186–197, 2018.

[3] S. Maleki, "Effect of deck and support stiffness on seismic response of slab-girder bridges," *Engineering Structures*, vol. 24, no. 2, pp. 219–226, 2002.

[4] E. G. Dimitrakopoulos, "Seismic response analysis of skew bridges with pounding deck-abutment joints," *Engineering Structures*, vol. 33, no. 3, pp. 813–826, 2011.

[5] S. Maleki, "Modeling of continuous slab-girder bridges for seismic analysis," in *Proceedings of the 8th International Conference on Civil and Structural Engineering Computing*, Civil-Comp press, Leuven, Belgium, September 2001.

[6] J. D. Kelley, *Three Dimensional Finite Element Modeling Techniques and Their Effect on the Seismic Response of a Highly Skewed Multi-Span Bridge*, pp. 1–20, Drexel University College of Engineering, Philadelphia, PA, USA, 2005.

[7] J. He and A. J. Ye, "Seismic response of continuous skew bridges with pounding effect," *Journal of Central South University*, vol. 43, no. 4, pp. 1475–1481, 2012.

[8] M. Amjadian, A. Kalantari, and A. K. Agrawal, "Analytical study of the coupled motions of decks in skew bridges with the deck-abutment collision," *Journal of Vibration and Control*, vol. 24, no. 7, pp. 1300–1321, 2018.

[9] W Jun-wen, S. Xian, and L. I. Jian-zhong, "Study of rotation mechanism and skew degree influence of skewed simply-supported beam bridge under earthquake excitation," *Bridge Construction*, vol. 44, no. 3, pp. 32–37, 2014.

[10] L. U. Ming-qi, Y Qin-shan, and L Ying-yong, "Torsion effects of skew angles on skew bridges during earthquakes," *Journal of Harbin Engineering University*, vol. 33, no. 2, pp. 155–159, 2012.

[11] P. Kaviani, F. Zareian, and E. Taciroglu, "Performance-based seismic assessment of skewed bridges," in *Proceedings of the Pacific earthquake engineering research center*, Berkeley, CA, USA, November 2014.

[12] J. Y. Meng and E. M. Lui, "Refined stick model for dynamic analysis of skew highway bridges," *Journal of Bridge Engineering*, vol. 7, no. 3, pp. 184–194, 2002.

[13] J. Y. Meng and E. M. Lui, "Seismic analysis and assessment of a skew highway bridge," *Engineering Structures*, vol. 22, no. 11, pp. 1433–1452, 2000.

[14] Y. J. Xu, *Study on Earthquake Damage Mechanism and Seismic Design for Highway Skewed Girder Bridges*, Fuzhou University, Fuzhou, China, 2016.

[15] Engineering-Civil Engineering, "Findings in Civil engineering reported from university of Nevada (experimental studies on seismic response of skew bridges with seat-type Abutments I: shake table experiments)," *Journal of Engineering*, vol. 24, no. 10, pp. 1–12, 2019.

[16] Engineering-Civil Engineering, "Data on Civil engineering reported by researchers at university of Nevada (experimental studies on seismic response of skew bridges with seat-type Abutments Ii: results)," *Journal of Engineering*, 2019.

[17] Z Jun Ping and Z Fu Lin, "Shaking table test of bridge vibration isolation system(III)-Test structure analysis," *Earthquake Engineering and Engineering Vibration*, vol. 22, no. 2, pp. 136–142, 2002.

[18] L. I. Zong-xiang, Y. Zhang, and Q Yue Fu, "Shaking table test of impact response of isolated simply supported beam bridge under earthquake," *Earthquake Engineering and Engineering Vibration*, vol. 27, no. 2, pp. 152–157, 2007.

[19] Industry recommended standard of the People's Republic of China, *Detailed Rules for Anti-seismic Design of Highway Bridges*, People's Communications Press, Beijing, China, 2020.

[20] Transportation Industry Standard of the People's Republic of China, *Plate Rubber Bearing for Highway*, People's Communications Press, Beijing, China, 2019.

[21] L. Chun-guang, *Seismic Response and Seismic Performance Analysis of Bridge Structures*, China Construction Industry Press, Beijing, China, 2010.

[22] "Research on dynamic characteristics of composite towering structure," *International Journal of Applied Mechanics*, vol. 13, no. 8, 2021.

[23] Y. X. Qin, Z. Q. Zhang, J. P. Gu et al., "Customized non-uniform discrete variables coordinated optimization coupling nonlinear mechanical analysis on complex truss structure," *Iranian Journal of Science and Technology*, p. 12, 2021.

[24] B. Scott, R. Park and M. Priestley, Stress-strain behavior of concrete confined by overlapping hoops at low and high strain rates," *Aci Journal*, vol. 79, no. 1, pp. 13–27, 1982.

[25] F. Taucer, E. Spacone, and F. C. Filippou, "A fiber beam-column element for seismic response analysis of reinforced concrete structures," University of California, Oakland, CA, USA, 1991.

[26] M. J. N. Priestle and F. Seible, *Seismic Design and Retrofit of bridge*, Wiley-Interscience, Hoboken, NJ, USA, 1996.

[27] S. Muthukumar and R. DesRoches, "Evaluation of Impact Models for Seismic pounding," in *Proceedings of the 13th World Conference on Earthqnake Engineering*, Vancouver, Canada, August 2004.

[28] G. Y. Zhang, *Bridge Structure test*, People's Communications Press, Beijing, China, 2002.

[29] Y. Lu, Y. Song, Y. Wang, and Y. Jiale, "Three-dimensional nonlinear seismic response of shield tunnel spatial end structure," *Advances in Civil Engineering*, vol. 2021, Article ID 8441325, 17 pages, 2021.